Periodic-Chaotic Sequences in a Detailed Mechanism of the Peroxidase-Oxidase Reaction

Baltazar D. Aguda† and Raima Larter*

Contribution from the Department of Chemistry, Indiana University-Purdue University at Indianapolis, Indianapolis, Indiana 46205. *Received February 20, 1991*

Abstract: Computer simulations of a detailed mechanism of the peroxidase-oxidase reaction show periodic-chaotic sequences for some ranges of enzyme concentrations. The mechanism involves two coupled feedback cycles that are both driven by oxygen. One of these cycles is the peroxidase catalytic cycle while the other is a conservation cycle involving all five known intermediates of the peroxidase enzyme. The reactions involving the enzyme intermediate ferroperoxidase are essential in generating complex and chaotic oscillations. This work demonstrates that the chaos previously observed in experiments can be accounted for by the known mechanism and kinetics of the reaction.

Introduction

We refer to the aerobic oxidation of nicotinamide adenine dinucleotide (NADH) catalyzed by the enzyme horseradish peroxidase (HRP) as the peroxidase-oxidase (PO) reaction. The overall stoichiometry of this reaction is

$$2NADH + O_2 + 2H^+ \rightarrow 2NAD^+ + 2H_2O \quad (1)$$

A typical experimental setup used in the study of this reaction involves blowing oxygen gas and slowly infusing NADH into a well-stirred solution of the enzyme HRP in an acidic buffer.[1] In 1977, Olsen and Degn[2] first reported their experimental observation of chaotic oscillations in the PO reaction. This observation was added to the growing list of nonlinear phenomena already exhibited by this reaction. These include multiple steady state[3] and damped[4] and sustained[5] oscillations. Recently, bistability between oscillatory behavior and steady state has also been demonstrated experimentally.[6]

Several models have been proposed for the peroxidase reaction. Notably, Olsen and Degn[1,7] proposed two abstract four-species models that have been shown capable of reproducing, qualitatively, the periodic and chaotic oscillations observed experimentally. More detailed models, based on known or postulated elementary steps, have also been proposed. Aguda and co-workers[8,9] have proposed a mechanism that accounts for the multiple steady states and oscillations. In addition, the bistability between oscillations and steady state was predicted prior to actual observation from simulations using the model proposed in ref 9. These latter calculations, in fact, stimulated the experimental search for this behavior. Fed'kina et al. have also proposed a detailed mechanism that reproduces the oscillations and have studied several other alternative schemes to account for various experimental features.[10-12] In this paper, we propose a detailed mechanism that exhibits complex and chaotic oscillations.

The Mechanism

A. The Importance of Ferroperoxidase. In a previous paper,[9] we showed that a PO mechanism we called model A exhibits sustained oscillations. Model A includes those reactions given in Table I except R_{11}, R_{12}, and R_{13}. So far we have not found any complex oscillations or chaos in simulations with model A. In our previous paper, we suggested[9] that including the enzyme intermediate ferroperoxidase, Per^{2+}, in the model would generate mixed-mode and chaotic oscillations. The key idea is that including Per^{2+} would introduce an additional feedback cycle, driven by oxygen. The importance of an additional cycle to the existence of chaos via this mechanism was also inferred from our studies of the chaotic four-species models.[13-16] Model A was therefore extended to include reactions R_{12}, producing Per^{2+}, and R_{13}, the reaction between Per^{2+} and O_2 (see Figure 1). In addition, the NADH concentration is now considered a dynamical variable and R_{11} is added to model the flow of NADH into the reactor (to conform with the experimental conditions). We shall refer to the network given in Figure 1 as model C.

B. The Kinetic Equations. When the reaction is held at constant temperature and well-stirred so as to produce spatially homogeneous conditions, the time evolution of the chemical species concentrations are given by the following set of differential equations:

$$\frac{dX_i}{dt} = \sum_{j=1}^{13} \nu_{ij} v_j \qquad i = 1, \ldots 10 \quad (2)$$

where X_i is the concentration of the ith species, v_j is the rate expression for the jth reaction, and ν_{ij} is equal to the stoichiometric coefficient of the ith species on the product side minus that on the reactant side of the jth reaction. The 13 reaction velocities v_j are given in Table I, while the species label "i" runs over the 10 chemical species, enumerated as shown in Figure 1.

For our present model, only 9 of the 10 chemical species are independent dynamical variables because the total enzyme concentration is always constant, i.e.

$$[Per^{2+}] + [Per^{3+}] + [col] + [colI] + [colII] = E_t \quad (3)$$

where the left hand side is the sum of the concentrations of the five enzyme intermediate species and E_t is the total enzyme concentration, a constant. We therefore have a total of 14 parameters (13 rate constants and 1 conservation constraint) in the kinetic equations of this model.

As given in the third column of Table I, the pseudoreactions

* Author to whom correspondence should be addressed.
† Present address: Department of Chemistry, York University, North York, Ontario, Canada M3J 1P3.

(1) Degn, H.; Olsen, L. F.; Perram, J. *Ann. N.Y. Acad. Sci.* **1979**, *316*, 623.
(2) Olsen, L. F.; Degn, H. *Nature* **1977**, *267*, 177.
(3) Degn, H. *Nature* **1968**, *217*, 1047.
(4) Yamazaki, I.; Yokota, K.; Nakajima, R. *Biochem. Biophys. Res. Commun.* **1965**, *21*, 582.
(5) Nakamura, S.; Yokota, K.; Yamazaki, I. *Nature* **1969**, *222*, 794.
(6) Aguda, B. D.; Hoffmann-Frisch, L.-L.; Olsen, L. F. *J. Am. Chem. Soc.* **1990**, *112*, 6652.
(7) Olsen, L. F. *Phys. Lett.* **1983**, *A94*, 454.
(8) Aguda, B. D.; Clarke, B. L. *J. Chem. Phys.* **1987**, *87*, 3461.
(9) Aguda, B. D.; Larter, R. *J. Am. Chem. Soc.* **1990**, *112*, 2167.
(10) Fed'kina, V.; Bronnikova, T.; Ataullakhanov, F. *Stud. Biophys.* **1981**, *82*, 159.
(11) Fed'kina, V.; Ataullakhanov, F.; Bronnikova, T. *Biophys. Chem.* **1984**, *19*, 259.
(12) Recently, V. Fed'kina and T. Bronnikova have developed a detailed PO mechanism that reportedly exhibits chaos (personal communication).
(13) Larter, R.; Bush, C. L.; Lonis, T. R.; Aguda, B. D. *J. Chem. Phys.* **1987**, *87*, 5765.
(14) Larter, R.; Steinmetz, C. G.; Aguda, B. D. *J. Chem. Phys.* **1988**, *89*, 6506.
(15) Aguda, B. D.; Larter, R.; Clarke, B. L. *J. Chem. Phys.* **1989**, *90*, 4168.
(16) Steinmetz, C. G.; Larter, R. *J. Chem. Phys.* **1991**, *94*, 1388.

0002-7863/91/1513-7913$02.50/0

Table I. Reactions in Model C and Rate Constants Used in the Simulations of Figure 3[a]

no.	reaction	reaction rate, v_j	rate constant, k_j
R_1	$Per^{3+} + H_2O_2 \rightarrow$ coI	$k_1[Per^{3+}][H_2O_2]$	10^6 M^{-1} s^{-1}
R_2	coI + NADH $\rightarrow$ coII + NAD$^\bullet$	k_2[coI][NADH]	10^6 M^{-1} s^{-1}
R_3	coII + NADH $\rightarrow Per^{3+}$ + NAD$^\bullet$	k_3[coII][NADH]	10^6 M^{-1} s^{-1}
R_4	coIII + NAD$^\bullet \rightarrow$ coI + $NADH^+$	k_4[coIII][NAD$^\bullet$]	10^6 M^{-1} s^{-1}
R_5	$Per^{3+} + O_2^- \rightarrow$ coIII	$k_5[Per^{3+}][O_2^-]$	6.0×10^7 M^{-1} s^{-1}
R_6	NAD$^\bullet + O_2 \rightarrow NAD^+ + O_2^-$	k_6[NAD$^\bullet$][O_2]	10^6 M^{-1} s^{-1}
R_7	$H^+ + O_2^- +$ NADH $\rightarrow H_2O_2$ + NAD$^\bullet$	$k_7[O_2^-]$[NADH]	10^6 M^{-1} s^{-1}
R_8	2NAD$^\bullet \rightarrow$ ( )	k_8[NAD$^\bullet$]^2	10^6 M^{-1} s^{-1}
R_9	( ) $\rightarrow O_2$	$k_t[O_2]_{eq} = 10^{-7}$ M s^{-1}	
R_{10}	$O_2 \rightarrow$ ( )	$k_t[O_2]$	$k_t = 0.1$ s^{-1}
R_{11}	( ) $\rightarrow$ NADH	10^{-7} M s^{-1}	
R_{12}	Per^{3+} + NAD$^\bullet \rightarrow Per^{2+}$ + NAD^+	$k_{12}[Per^{3+}][NAD^\bullet]$	10^6 M^{-1} s^{-1}
R_{13}	$Per^{2+} + O_2 \rightarrow$ coIII	$k_{13}[Per^{2+}][O_2]$	10^6 M^{-1} s^{-1}

[a] Abbreviations: Per^{3+}, ferriperoxidase; coI, compound I; coII, compound II; coIII, compound III; Per^{2+}, ferroperoxidase; NADH, nicotinamide adenine dinucleotide.

R_9 and R_{10} correspond to the two terms in the rate of diffusion of oxygen gas across the gas/liquid phase boundary:[1,2]

$$\text{diffusion rate} = k_t\{[O_2]_{eq} - [O_2]\} = v_9 - v_{10} \qquad (4)$$

where $[O_2]_{eq}$ is the concentration of dissolved oxygen when equilibrated with the gas phase, $[O_2]$ is the liquid-phase nonequilibrium concentration, and k_t is the oxygen phase-transfer rate constant, which will be partly determined by the stirring rate. We let $v_9 = k_t[O_2]_{eq}$ and $v_{10} = k_t[O_2]$.

In determining the dynamics of the model, the relative magnitudes of the rate constants are more important than their individual absolute values. The relationships between the rate constants can be given in terms of ratios appearing in a dimensionless form of the kinetic equations. Dedimensionalization of the kinetic equations is not a unique procedure and depends on the scaling chosen. One set of equations that results from a particular choice of scaling is given below.

$$\epsilon_a \frac{da}{d\tau} = cn - aw$$

$$\epsilon_b \frac{db}{d\tau} = (c + x + y)n - (f + w + z)b - 2\gamma b^2$$

$$\epsilon_c \frac{dc}{d\tau} = bf - (n + w)c \qquad \frac{df}{d\tau} = 1 - (1 + b + v)f$$

$$\epsilon_n \frac{dn}{d\tau} = \alpha - (c + x + y)n \qquad \epsilon_w \frac{dw}{d\tau} = yn - (a + b + c)w$$

$$\epsilon_x \frac{dx}{d\tau} = bz + aw - xn \qquad \epsilon_y \frac{dy}{d\tau} = (x - y)n$$

$$\epsilon_z \frac{dz}{d\tau} = cw + vf - bz \qquad \epsilon_v \frac{dv}{d\tau} = bw - vf \qquad (5a)$$

where we have defined the following variables:

$$\tau = k_{10}t \qquad a = \frac{k_1 k_6 A}{k_{10} k_{12}}$$

$$b = \frac{k_6 B}{k_{10}} \qquad c = \frac{k_5 k_6 C}{k_{10} k_{12}}$$

$$f = \frac{k_{10} F}{k_9} \qquad n = \frac{k_7 k_{10} k_{12} N}{k_5 k_6 k_9}$$

$$w = \frac{k_{10} k_{12} W}{k_6 k_9} \qquad x = \frac{k_2 k_5 k_6 X}{k_7 k_{10} k_{12}}$$

$$y = \frac{k_3 k_5 k_6 Y}{k_7 k_{10} k_{12}} \qquad z = \frac{k_4 k_{10} Z}{k_6 k_9} \qquad v = \frac{k_{13} V}{k_{10}}$$

$$A = [H_2O_2] \qquad B = [NAD^\bullet] \qquad C = [O_2^-]$$

$$F = [O_2] \qquad N = [NADH]$$

$$W = [Per^{3+}] \qquad X = [coI] \qquad Y = [coII]$$

$$Z = [coIII] \qquad V = [Per^{2+}] \qquad (5b)$$

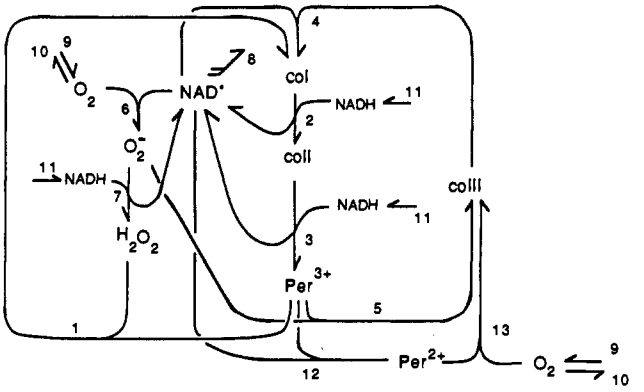

Figure 1. Network diagram of the peroxidase–oxidase mechanism exhibiting chaos, model C. Only the dynamical species are shown; the details of the reaction steps are given in Table I.

Here, the parameters that relate the rate constants to one another are the scaling coefficients:

$$\epsilon_a = \frac{k_{10}^2 k_{12}}{k_1 k_6 k_9} \qquad \epsilon_b = \frac{k_{10}^2}{k_6 k_9}$$

$$\epsilon_c = \frac{k_{10}^2 k_{12}}{k_5 k_6 k_9} \qquad \epsilon_n = \frac{k_5 k_6}{k_7 k_{12}}$$

$$\epsilon_y = \frac{k_7 k_{10}^2 k_{12}}{k_3 k_5 k_6 k_9} \qquad \epsilon_x = \frac{k_7 k_{10}^2 k_{12}}{k_2 k_5 k_6 k_9}$$

$$\epsilon_v = \frac{k_{10}^2}{k_9 k_{13}} \qquad \gamma = \frac{k_8 k_{10}^2}{k_9 k_6^2}$$

$$\epsilon_w = \frac{k_6}{k_{12}} \qquad \epsilon_z = \frac{k_6}{k_4} \qquad \alpha = \frac{k_{11}}{k_9} \qquad (5c)$$

The rate constants used in our simulations correspond to $\epsilon_a = \epsilon_b = \epsilon_v = \gamma = 0.1$, $\epsilon_w = \epsilon_z = \alpha = 1.0$, $\epsilon_c = \epsilon_x = \epsilon_y = 0.001\,67$, and $\epsilon_n = 60$. With this choice of parameter values, NADH is a slowly varying species while O_2^-, coI, and coII are fast species. This separation of time scales is consistent with the conditions for complex oscillations and chaos we found in our study of one of the simple four-variable models for this reaction.[14]

Results

A. Hopf Bifurcation Values. The first step in finding the parameters that give chaos is to determine the set of parameters that lead to oscillations. In Figure 2a, the dotted curve represents the Hopf bifurcation points[17] that delineate values of v_9 and E_t that give oscillations from those that do not. We have chosen to focus on these two parameters here because one can conceive of

(17) Hassard, B.; Kazarinoff, N.; Wan, Y.-H. *Theory and Applications of Hopf Bifurcation*; Cambridge University Press: London, 1981.

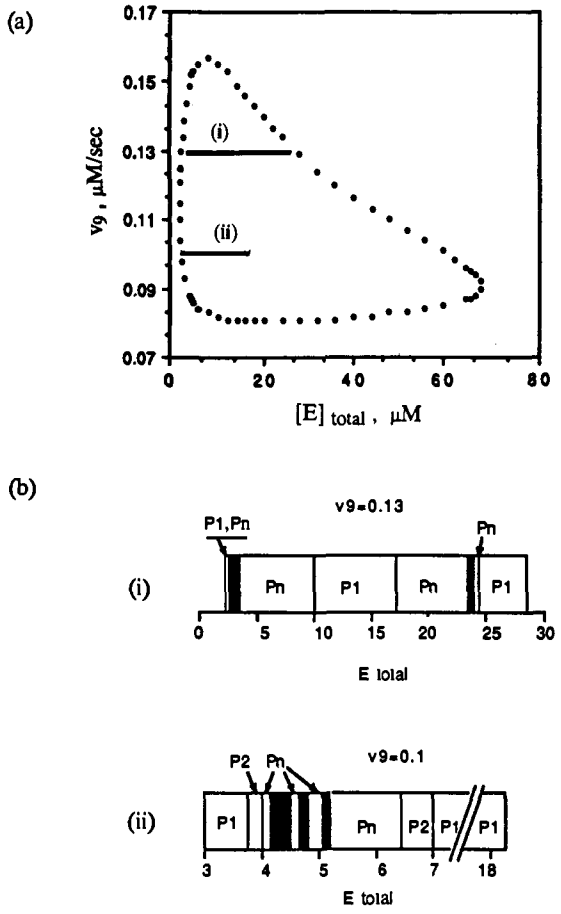

Figure 2. (a) Area enclosed by the dotted curve: region of oscillations (chaotic or otherwise) on the $v_9 - E_t$ parameter plane, where v_9 is the rate of oxygen gas input defined in Table I and E_t is the total enzyme concentration. The dotted curve represents Hopf bifurcation points. The fixed values of the other parameters are given in Table I. (b) Character of the oscillations observed corresponding to the parameters found in line segments i and ii in (a). The black bars represent chaotic windows; P1 = period-one limit cycle oscillations; P2 = period-two oscillations; Pn = region with period-doubling cascade.

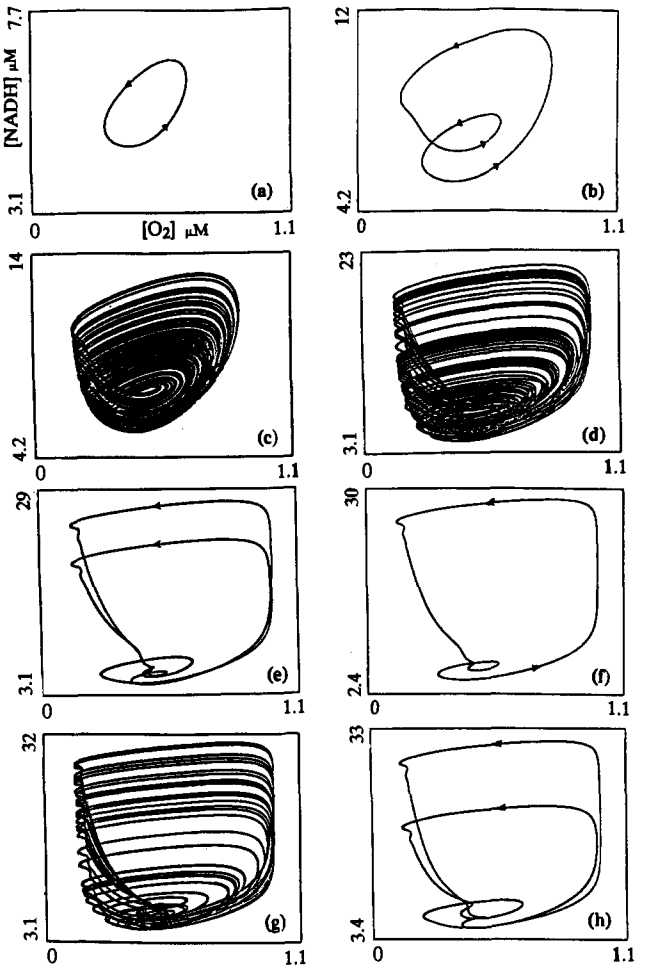

Figure 3. Dynamics of the PO reaction model on the [NADH] – [O_2] concentration plane for $v_9 = 0.1$ and the following total enzyme concentrations E_t (μM): (a) 3.0, (b) 4.0, (c) 4.2, (d) 4.3, (e) 4.8, (f) 4.9, (g) 5.1, and (h) 5.2. The other parameter values are given in Table I. All integrations were done by using LSODE (ref 18). In all cases, the initial conditions are (μM) $[H_2O_2] = 1.27 \times 10^{-3}$, $[NAD^{\bullet}] = 3.18 \times 10^{-2}$, $[O_2^-] = 4.84 \times 10^{-4}$, $[O_2] = 0.758$, [NADH] = 2.09, $[Per^{3+}] = 0.76$, [coI] = 0.02, [coII] = 0.02, [coIII] = 1.40, $[Per^{2+}] = E_t - \{[Per^{3+}] + [coI] + [coII] + [coIII]\}$. The trajectories shown are plotted after allowing transients to die away, usually by neglecting the first 10^4 or 10^5 time units after the start.

experimental means to vary v_9 (through the stirring rate and oxygen pressure) as well as E_t, the total enzyme concentration. We see in Figure 2 that there exists a closed region in the $v_9 - E_t$ parameter plane where oscillations can occur. We find that these oscillations can be complex and even chaotic within certain regions, as described in more detail in the following section.

B. Periodic–Chaotic Sequences. Computer simulations were carried out by using parameter values found along the line segments i and ii shown in Figure 2a, corresponding to $v_9 = 0.1$ and $v_9 = 0.13$, respectively. The LSODE implementation of the Gear algorithm was used.[18] For $v_9 = 0.13$, we found two windows of chaos indicated by the black bars in Figure 2b,i. For $v_9 = 0.1$, three windows of chaos were found as shown in Figure 2b,ii. Examples of the phase space trajectories in the latter region of parameter space are given in Figure 3. In Figure 3a, the first Hopf bifurcation point has just been crossed and we see a simple one-loop limit cycle. As E_t is increased to 4.2, a cascade of period doubling occurs (indicated by Pn in Figure 2b,ii; see also Figure 3b) until, at $E_t = 4.2$, chaos is observed (see Figure 3c,d). The first chaotic region was found to be quite large, extending from $E_t = 4.19$ to 4.52. Between $E_t = 4.52$ and 4.60, periodic states are again found. Chaotic oscillations reappear between $E_t = 4.65$ and 4.75. Periodic states are found between $E_t = 4.8$ and 5.05 (see Figure 3e,f), and a small window of chaos is observed between $E_t = 5.08$ and 5.15 (see Figure 3g). For E_t values higher than 5.1, a reverse period-doubling sequence is found (see Figure 3h) that culminates in a limit cycle.

The next-amplitude maps for the chaotic states of Figure 3c,d are shown in Figure 4a,b, respectively. The map shown in Figure 4a is almost single branched while that in Figure 4b has at least five branches. The single hump associated with the map of Figure 4a indicates that the chaotic dynamics for this state (found near the onset of chaos) can be described in terms of a single variable, or possibly two. As the chaos becomes more highly developed (Figure 4b), the number of variables needed for its complete description increases, leading to a multiple-branched next-amplitude map.

Discussion

The necessary conditions for the existence of chaos in the peroxidase–oxidase reaction include the following: (1) at least two feedback cycles must be present in the mechanism; and (2) a separation of time scales must exist. These conclusions can be drawn from our extensive previous studies of the detailed mechanism, as well as the simpler four-species models, and have been further refined by the current work. The results presented here allow us to be more precise about these necessary conditions.

More specifically, we have found that the two feedback cycles are (i) the peroxidase catalytic cycle corresponding to reactions R_1, R_2, R_3, R_6, and R_7, in which $NAD^{\bullet}$ is the key intermediate;

(18) Hindmarsh, A. C. *ACM Signum Newsletter* **1980**, *15*, 10.

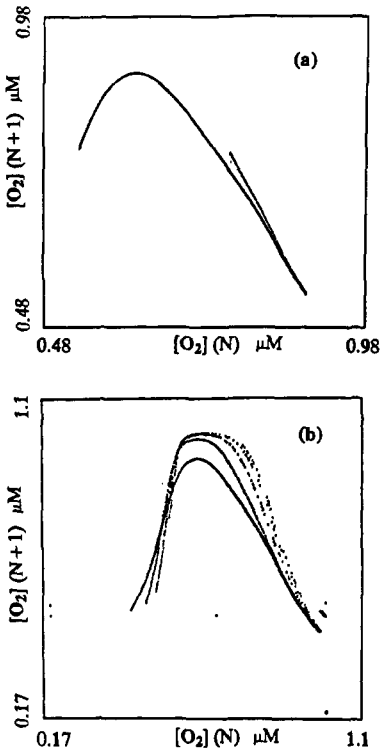

Figure 4. Next-amplitude maps corresponding to the dynamical trajectories shown in Figure 3c,d.

and (ii) a second cycle involving all five enzyme intermediate species, reactions R_2, R_3, R_{12}, R_{13}, and R_4. Both of these cycles are driven by external feeds of oxygen and NADH and have the reaction steps R_2 and R_3 in common. Since the two cycles are intimately connected through the two steps R_2 and R_3, but still operate somewhat separately, complex oscillations and chaos can result when the oscillations produced by one cycle interact with those due to the other cycle.

In addition, the necessary separation of time scales is always found to involve NADH as the slowly varying species. The results of the present study indicate that the fast species in the mechanism include two of the enzyme intermediates (col and col1) as well as $O_2^{\cdot-}$. Previous studies of the simple four-variable models of the reaction indicated that NADH was a slow variable whose sluggish changes drive the fast variables over a folded manifold. When these fast variables pass through bifurcation points, the full system responds with oscillations of differing magnitudes, resulting in complex periodic or chaotic dynamics.

Clues as to the nature of the chaotic behavior seen in the reaction can also be found by studying the routes to chaos as a system parameter is varied. Two examples have been described and are illustrated in Figure 3. The sequence corresponding to Figure 3a to b to c shows a period-doubling route leading to a strange attractor that is similar in appearance to the Lorenz attractor. At higher enzyme concentrations, another type of period-doubling sequence leads to the strange attractor shown in Figure 3g, which seems to have an unstable focus near the lower left side. The complex periodic states in nearby regions of parameter space (such as that shown in Figure 3f) are of the mixed-mode type, i.e., composed of combinations of clearly distinguishable large-amplitude and small-amplitude oscillations. The route by which chaos arises in this mixed-mode region also involves a period-doubling sequence.

Recently, we have carried out detailed studies of one of the four-variable models[16] which showed that mixed-mode oscillations can arise when a torus attractor wrinkles, becomes fractal, and eventually breaks up. Once the torus breakup has occurred, mixed-mode oscillations are found to occur in a Farey-sequence order. The periodic mixed-mode oscillations undergo period-doubling bifurcations resulting in chaos[16,19] in much the same manner as seen here for this more detailed mechanism. The existence of Farey sequences or an underlying torus in the more detailed model has not yet been confirmed. However, the striking similarities between the dynamics of these two mechanisms indicate that it might be worthwhile to search for such behavior by continuing with further simulations of model C.

The explanations put forth here for the emergence of chaos in the peroxidase–oxidase reaction are remarkably similar to one scenario proposed for chemical chaos in the Belousov–Zhabotinskii reaction.[20] In that reaction, multiple time scales and coupled feedback loops have also been implicated by extensive experimental and theoretical studies. In order to determine whether these conclusions are generally true for all examples of chemical chaos, more examples must be studied. The implications of our results, though, are that this single explanation of chemical chaotic behavior, which has now been established for two quite distinctly different reactions, will carry over to yet-to-be-discovered examples of chemical chaos.

Conclusions

We have shown that a detailed mechanism of the peroxidase reaction, based on known biochemical pathways that occur in vivo, can sustain complex oscillations and chaos. The chaotic dynamics are seen to arise via a period-doubling route and are associated with a strange attractor that is similar in appearance to the Lorenz attractor for some enzyme concentrations. At higher enzyme concentrations, the existence of an unstable focus in the strange attractor seems to be associated with nearby mixed-mode periodic states. The existence of chaos depends on the inclusion of two reactions involving the enzyme intermediate ferroperoxidase, Per^{2+}, in a previously suggested mechanism. Without these additional reactions, the detailed mechanism (model A of ref 9) supported multiple steady states and sustained, but not complex, oscillations. The added reactions correspond to an additional feedback cycle, known to be a necessary condition for the existence of complex oscillations and chaos in the simple four-variable models for the peroxidase–oxidase oscillator. In the current model, this additional feedback cycle is driven by oxygen and NADH, reactants that are continuously fed into the system.

Some possible problems remain with the current mechanism. These include some uncertainty in the values of the rate constants used. Conflicting values are reported in the literature in some cases.[9] Even though it is important to consider only the crucial ratios, as given in eq 5, it is still important to start with the best possible known values of the rate constants. One reason for the confusion in the literature is that rate "constants" as reported are sometimes actually pseudo rate constants which depend on concentrations of constant species or the pH. In this situation, it is difficult to compare one set of experimentally determined rate constants with another, especially if the experimental conditions are not completely specified. Another, possibly minor, problem involves the order of the termination reaction for NAD•, reaction R_8, which here is taken to be second order. It might be better to model this termination as a first-order reaction, since it may occur via collision of the radicals with the walls of the reaction vessel.[21] Whether such a change would have any effect on the oscillatory behavior of this mechanism is unknown at this point. More studies, both experimental and computational, are needed in order to elucidate the true origin of chaos in the peroxidase–oxidase oscillating reaction.

Acknowledgment. This research has been supported by the National Science Foundation (Grant No. CHE-8913895) and the Petroleum Research Fund, administered by the American Chemical Society. We are also grateful to Lars Folke Olsen of Odense University and Alexander Scheeline and Dean Olson of the University of Illinois for stimulating and informative discussions.

(19) Larter, R.; Steinmetz, C. G. *Philos. Trans. R. Soc. London, A*, in press.

(20) Barkely, D.; Ringland, J.; Turner, J. S. *J. Chem. Phys.* **1987**, *87*, 3812.

(21) A. Scheeline, personal communication.